Inorganic Chemistry

Article

pubs.acs.org/IC

Cation Size Effect on the Framework Structures in a Series of New Alkali-Metal Indium Selenites, $AIn(SeO_3)_2$ (A = Na, K, Rb, and Cs)

Dong Woo Lee, Saet Byeol Kim, and Kang Min Ok*

Department of Chemistry, Chung-Ang University, 221 Heukseok-dong, Dongjak-gu, Seoul 156-756, Republic of Korea

Supporting Information

ABSTRACT: A new family of quaternary alkali-metal indium selenites, $AIn(SeO_3)_2$ (A = Na, K, Rb, and Cs) have been synthesized, as crystals and pure polycrystalline phases through standard solid-state and hydrothermal reactions. The structures of the reported materials have been determined by single-crystal X-ray diffraction. While $AIn(SeO_3)_2$ (A = Na, K, and Rb) crystallize in the orthorhombic space group, *Pnma*, with three-dimensional framework structures, $CsIn(SeO_3)_2$ crystallizes in the trigonal space group, $R\bar{3}m$, with a two-dimensional structure. All of the reported materials, however, share a common structural motif, a network of corner-shared InO_6 octahedra and SeO_3 groups. Interestingly, the size of the alkali-metal cations profoundly influences the bonding nature of the SeO_3 group to the InO_6 octahedra. Complete characterizations including infrared spectroscopy, elemental analyses, and thermal analyses for the compounds are also presented, as are dipole moment calculations. A detailed cation size effect on the framework structure is discussed.

INTRODUCTION

Mixed-metal selenite (Se^{4+}) materials have attracted a great deal of attention, attributed to their particular type of functional characteristics such as second-order nonlinear optical (NLO) properties, piezoelectricity, pyroelectricity, and ferroelectricity.[1−4] The technologically important properties are closely related to crystallographic noncentrosymmetry (NCS), which can be achieved in an easy manner from the combination of the inherent local asymmetric coordination environment with stereoactive lone pairs.[5−7] With oxide materials, the lone pairs creating an asymmetric coordination environment are considered to be the result of a second-order Jahn−Teller (SOJT) distortion.[8−12] A list of SOJT distortive lone-pair cations includes Tl^+, Sn^{2+}, Sb^{3+}, Se^{4+}, Te^{4+}, and I^{5+}.[13] In addition, materials containing cations with nonbonded electron pair can exhibit a rich structural chemistry inasmuch as the cations can adopt variable coordination geometry.[14,15] Furthermore, once the variable coordination environment of the lone-pair cations is combined with other structurally flexible cations such as p-elements, a great deal of interesting structural features can be synergistically obtained. With these ideas in mind, we decided to investigate the A^+−In^{3+}−Se^{4+} oxide system. Although the In^{3+} cation, as a p-element, can form a larger and stable octahedral coordination environment with greater flexibility, Se^{4+} inherently possesses asymmetric structural geometry attributed to the nonbonded electron pair. In fact, several indium selenites materials such as $Cs_3H_6In_5(SeO_3)_{12}$,[16] $CsIn_3H_2(SeO_3)_6(H_2O)_2$,[17] $In(HSeO_3)(SeO_3)$,[18] $In(HSeO_3)_3(H_2O)_3$,[19] $In_2(Se_2O_5)_3$,[20] $In(OH)(SeO_3)$,[21] $In_2Cu_3(SeO_3)_6$,[22] $[In_2(SeO_3)_2(C_2O_4)(H_2O)_2]\cdot 2H_2O$,[23] $In_2Mo_2Se_2O_{13}(H_2O)$,[24] $InSeO_3Cl$,[25] and $InVSe_2O_8$[26] have been reported. Among them, $In_2(Se_2O_5)_3$[20] and $InVSe_2O_8$[26] crystallize in NCS framework structures and exhibit SHG efficiencies of 10 and 30 times that of α-SiO_2, respectively. Also, $Cs_3H_6In_5(SeO_3)_{12}$[16] and $CsIn_3H_2(SeO_3)_6(H_2O)_2$[17] show three-dimensional CS framework structures. Here, we report a new family of quaternary alkali-metal indium selenites, $AIn(SeO_3)_2$ (A = Na, K, Rb, and Cs). Complete structural analysis, infrared spectra, elemental analyses, thermal analyses, and dipole moment calculations of the reported materials are presented. We also demonstrate that the cation size significantly influences the framework structures of the stoichiometrically equivalent materials.

EXPERIMENTAL SECTION

Reagents. Na_2CO_3 (Hayashi, 99.5%), K_2CO_3 (Jin Chemical, 99.5%), Rb_2CO_3 (Acros, 99.5%), Cs_2CO_3 (Aldrich, 99.0%), In_2O_3 (Alfa Aesar, 99.9%), $In(NO_3)_3\cdot xH_2O$ (Alfa Aesar, 99.99%), and SeO_2 (Aldrich, 98%) were used as received. $NaInO_2$ and $KInO_2$ were synthesized via standard solid-state reactions. A stoichiometric amount of A_2CO_3 (A = Na or K) and In_2O_3 was thoroughly ground and pressed into pellets. The respective pellets were heated to 800 °C for 24 h and cooled to room temperature.

Synthesis. Crystals of $NaIn(SeO_3)_2$ and $KIn(SeO_3)_2$ were prepared by standard solid-state reactions. For single crystals of $AIn(SeO_3)_2$ (A = Na and K), 2.00×10^{-3} mol of $AInO_2$ and 6.00×10^{-3} mol of SeO_2 were thoroughly mixed with agate mortars and pestles under an atmosphere of dry argon. The respective reaction mixtures were then introduced into fused silica tubes that were subsequently evacuated and sealed. Each tube was gradually heated to 380 °C for 5 h, 650 °C for 48 h, and cooled at a rate of 6 °C h^{-1} to room temperature. The products contained colorless block crystals of $AIn(SeO_3)_2$ (A = Na and K) with some unknown amorphous phases. Crystals of $RbIn(SeO_3)_2$ and $CsIn(SeO_3)_2$ were prepared by hydrothermal reactions. Quantities of Rb_2CO_3 or Cs_2CO_3 (3.00×10^{-3} mol), $In(NO_3)_3\cdot xH_2O$ (1.00×10^{-3} mol), SeO_2 (2.00×10^{-3} mol), and deionized water (2 mL) were combined. The respective reaction mixtures were transferred to Teflon-lined stainless steel autoclaves. The autoclaves were then subsequently sealed and heated to 230 °C, held for 4 days, and cooled at a rate of 6 °C h^{-1} to room temperature. After cooling, the autoclaves were opened and the products were recovered by filtration and washed with distilled water.

Received: May 26, 2012
Published: July 16, 2012

   dx.doi.org/10.1021/ic301316r | *Inorg. Chem.* 2012, 51, 8530−8537

Table 1. Crystallographic Data for $AIn(SeO_3)_2$ (A = Na, K, Rb, and Cs)

formula	$NaInSe_2O_6$	$KInSe_2O_6$	$RbInSe_2O_6$	$CsInSe_2O_6$
fw	391.73	407.84	454.21	501.65
space group	*Pnma* (No. 62)	*Pnma* (No. 62)	*Pnma* (No. 62)	$R\bar{3}m$ (No. 166)
a	12.8301(12) Å	13.1567(4) Å	15.8420(11) Å	5.62560(10) Å
b	5.4382(5) Å	5.5511(2) Å	5.5594(4) Å	5.62560(10) Å
c	8.1707(9) Å	8.3381(3) Å	7.6158(5) Å	19.3357(5) Å
V	570.09(10) $Å^3$	608.97(4) $Å^3$	670.74(8) $Å^3$	529.942(19) $Å^3$
Z	4	4	4	3
T	200.0(2) K	200.0(2) K	200.0(2) K	200.0(2) K
λ	0.71073 Å	0.71073 Å	0.71073 Å	0.71073 Å
ρ_{calcd}	4.564 g cm^{-3}	4.448 g cm^{-3}	4.498 g cm^{-3}	4.716 g cm^{-3}
μ	16.952 mm^{-1}	16.484 mm^{-1}	21.555 mm^{-1}	18.695 mm^{-1}
$R(F)^a$	0.0432	0.0318	0.0191	0.0347
$R_w(F_o^2)^b$	0.1218	0.0570	0.0442	0.0950

$^aR(F) = \sum||F_o| - |F_c||/\sum|F_o|$. $^bR_w(F_o^2) = [\sum w(F_o^2 - F_c^2)^2/\sum w(F_o^2)^2]^{1/2}$.

Table 2. Selected Bond Distances for $AIn(SeO_3)_2$ (A = Na, K, Rb, and Cs)

	bond distance (Å)	bond valence		bond distance (Å)	bond valence
	$NaIn(SeO_3)_2$			**$KIn(SeO_3)_2$**	
In(1)−O(1) × 2	2.143(7)	0.507	In(1)−O(1) × 2	2.160(4)	0.483
In(1)−O(2)	2.162(11)	0.481	In(1)−O(2)	2.167(5)	0.474
In(1)−O(3) × 2	2.166(6)	0.475	In(1)−O(3) × 2	2.164(4)	0.478
In(1)−O(4)	2.108(9)	0.560	In(1)−O(4)	2.113(5)	0.552
Bond Valence Sum of In(1)		3.005	Bond Valence Sum of In(1)		2.948
Se(1)−O(1) × 2	1.658(8)	1.399	Se(1)−O(1) × 2	1.698(4)	1.274
Se(1)−O(2)	1.668(10)	1.367	Se(1)−O(2)	1.704(6)	1.256
Bond Valence Sum of Se(1)		4.165	Bond Valence Sum of Se(1)		3.804
Se(2)−O(3) × 2	1.693(6)	1.289	Se(2)−O(3) × 2	1.690(4)	1.296
Se(2)−O(4)	1.700(9)	1.266	Se(2)−O(4)	1.678(5)	1.333
Bond Valence Sum of Se(2)		3.844	Bond Valence Sum of Se(2)		3.925
	$RbIn(SeO_3)_2$			**$CsIn(SeO_3)_2$**	
In(1)−O(1) × 2	2.134(2)	0.519	In(1)−O(1) × 6	2.153(4)	0.507
In(1)−O(2)	2.140(3)	0.512	Bond Valence Sum of In(1)		3.042
In(1)−O(3)	2.171(3)	0.469			
In(1)−O(4) × 2	2.177(2)	0.460	Se(1)−O(1) × 3	1.695(4)	1.394
Bond Valence Sum of In(1)		2.939	Se(1′)−O(1) × 3	1.623(6)	
			Bond Valence Sum of Se(1)^a		4.183
Se(1)−O(1) × 2	1.689(2)	1.300			
Se(1)−O(2)	1.687(3)	1.305			
Bond Valence Sum of Se(1)		3.905			
Se(2)−O(3)	1.695(3)	1.280			
Se(2)−O(4) × 2	1.694(2)	1.285			
Bond Valence Sum of Se(2)		3.850			

^{a}Since Se(1) and Se(1′) have fractional occupancies of 0.913(8) and 0.093(9), respectively, average bond valence sums are calculated.

Colorless crystals of $RbIn(SeO_3)_2$ and $CsIn(SeO_3)_2$ were obtained in yields of 21% and 31%, respectively, based on the corresponding metal carbonates. After determining the crystal structures, pure bulk polycrystalline samples of $AIn(SeO_3)_2$ (A = Na, K, Rb, and Cs) were synthesized through standard solid-state reactions with stoichiometric amounts of the starting materials. $AInO_2$ (2.00×10^{-3} mol) was thoroughly mixed with 4.00×10^{-3} mol of SeO_2 and pressed into pellets. The pellets were introduced into fused-silica tubes that were evacuated and subsequently sealed. Each tube was gradually heated to 550 °C for 24 h with an intermediate regrinding. The powder X-ray diffraction (XRD) patterns on the resultant polycrystalline products exhibited the materials were single phases and were in good agreements with the generated patterns from the single-crystal data (see the Supporting Information).

Single-Crystal X-ray Diffraction. The structures of $AIn(SeO_3)_2$ (A = Na, K, Rb, and Cs) were determined by standard crystallographic methods. A colorless rod (0.032 mm × 0.041 mm × 0.057 mm) for $NaIn(SeO_3)_2$, a colorless rod (0.010 mm × 0.020 mm × 0.035 mm) for $KIn(SeO_3)_2$, a colorless block (0.044 mm × 0.048 mm × 0.065 mm) for $RbIn(SeO_3)_2$, and a colorless hexagonal prism (0.021 mm × 0.067 mm × 0.101 mm) for $CsIn(SeO_3)_2$ were used for single-crystal data analyses. All of the data were collected using a Bruker SMART BREEZE diffractometer equipped with a 1K CCD area detector using graphite monochromated Mo Kα radiation at 200 K. A hemisphere of data was collected using a narrow-frame method with scan widths of

dx.doi.org/10.1021/ic301316r | *Inorg. Chem.* 2012, 51, 8530−8537

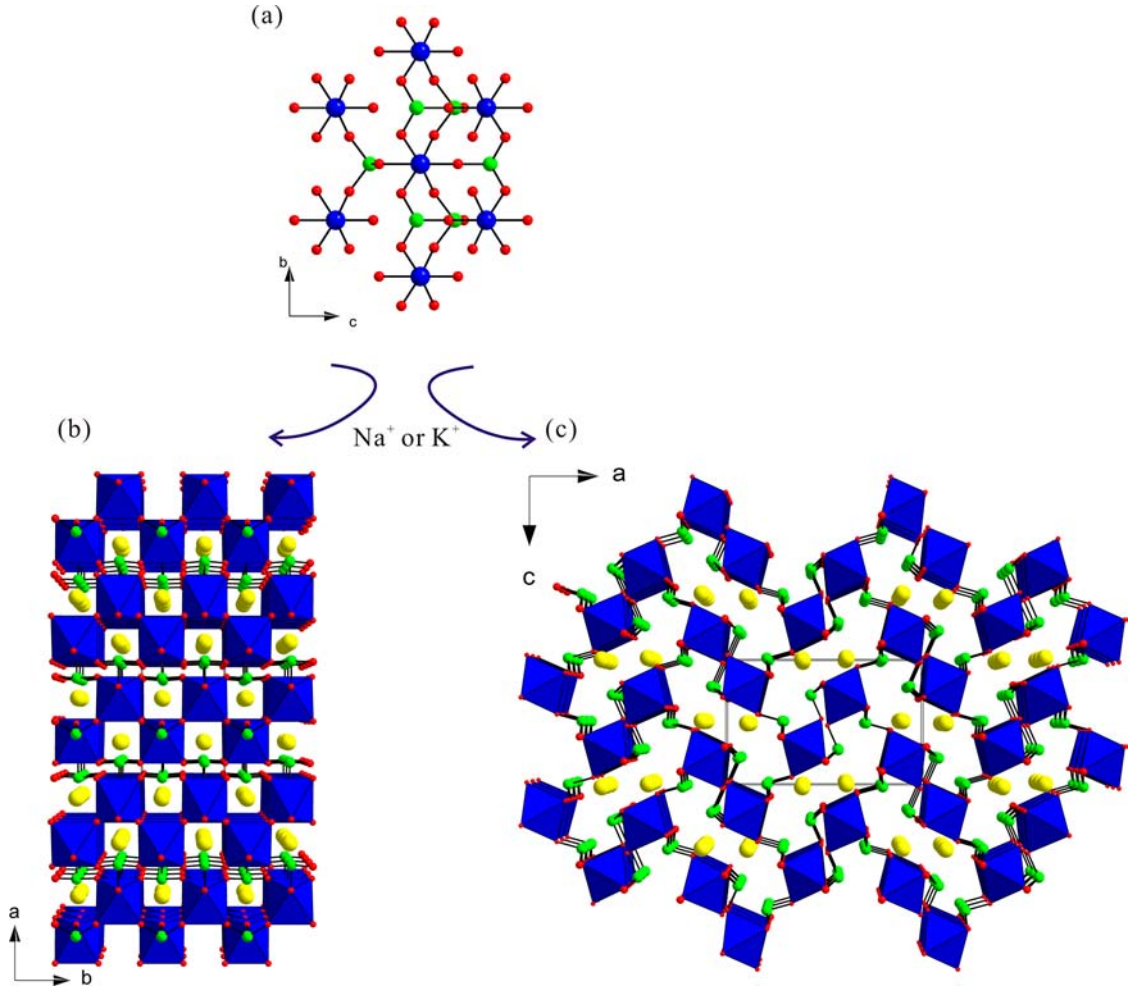

Figure 1. (a) Ball-and-stick and polyhedral representations of $NaIn(SeO_3)_2$ or $KIn(SeO_3)_2$ in the *bc*-plane. (b) Four-membered ring channels running along the [001] direction. (c) Twelve-membered ring channels composed of InO_6 octahedra and SeO_3 polyhedra running along the [010] direction (blue, In; green, Se; yellow, Na or K; red, O).

0.30° in omega, and an exposure time of 5 s/frame. The first 50 frames were remeasured at the end of the data collection to monitor instrument and crystal stability. The maximum correction applied to the intensities was <1%. The data were integrated using the SAINT program,[27] with the intensities corrected for Lorentz factor, polarization, air absorption, and absorption attributable to the variation in the path length through the detector faceplate. A semiempirical absorption correction was made on the hemisphere of data with the SADABS program.[28] The data were solved and refined using SHELXS-97[29] and SHELXL-97,[30] respectively. All calculations were performed using the WinGX-98 crystallographic software package.[31] Crystallographic data and selected bond distances with bond valence sums for the reported material are given in Tables 1 and 2. An examination of 16 examples of InO_6 octahedra exhibits that the In−O bond distances range from 2.073(4) Å to 2.359(10) Å with the average distance of 2.156 Å.[16−26] Also, an examination of 36 examples of SeO_3 polyhedra reveals that the Se−O bond lengths range from 1.552(10) Å to 1.806(33) Å with the average distance of 1.700 Å.[16−26] As can be seen in Table 2, all the In−O and Se−O bond distances for the reported materials are consistent with those of previously reported indium selenites materials.

Powder X-ray Diffraction. Powder X-ray diffraction (XRD) was used to confirm the phase purity for the synthesized materials. The powder XRD data were collected on a Bruker D8-Advance diffractometer using Cu Kα radiation at room temperature with 40 kV and 40 mA. The polycrystalline samples were mounted on sample holders and scanned in the 2θ range of 10−70° with a step size of 0.02°, and a step time of 0.2 s. The experimental powder XRD patterns are in good agreement with those calculated data from the single-crystal models.

Infrared Spectroscopy. Infrared spectra were recorded on a Varian 1000 FT-IR spectrometer in the 400−4000 cm^{-1} range, with the sample embedded in a KBr matrix.

Thermogravimetric Analysis. Thermogravimetric analysis (TGA) was performed on a Setaram LABSYS TG-DTA/DSC thermogravimetric analyzer. The polycrystalline samples were contained within alumina crucibles and heated at a rate of 10 °C min^{-1} from room temperature to 1000 °C under flowing argon.

Scanning Electron Microscopy/Energy-Dispersive Analysis by X-ray (SEM/EDAX). SEM/EDAX has been performed using a Hitachi Model S-3400N/Horiba Energy Model EX-250 instruments. EDAX for $AIn(SeO_3)_2$ (A = Na, K, Rb, and Cs) exhibit A/In/Se ratios of ∼1:1:2.

RESULTS AND DISCUSSION

Structures. $NaIn(SeO_3)_2$ and $KIn(SeO_3)_2$. $NaIn(SeO_3)_2$ and $KIn(SeO_3)_2$ are isostructual and crystallize in the centrosymmetric space group *Pnma* (No. 62). The materials are new quaternary A^+−In^{3+}−Se^{4+} oxides containing distorted InO_6 octahedra and asymmetric SeO_3 polyhedra connected by In−O−Se bonds. Interestingly, there are no In−O−In and Se−O−Se bonds. The In^{3+} cations are in a distorted octahedral coordination environment, bonded to six oxygen atoms (see Figure 1a). The In−O bond lengths range from 2.108(9) Å to

dx.doi.org/10.1021/ic301316r | *Inorg. Chem.* 2012, 51, 8530−8537

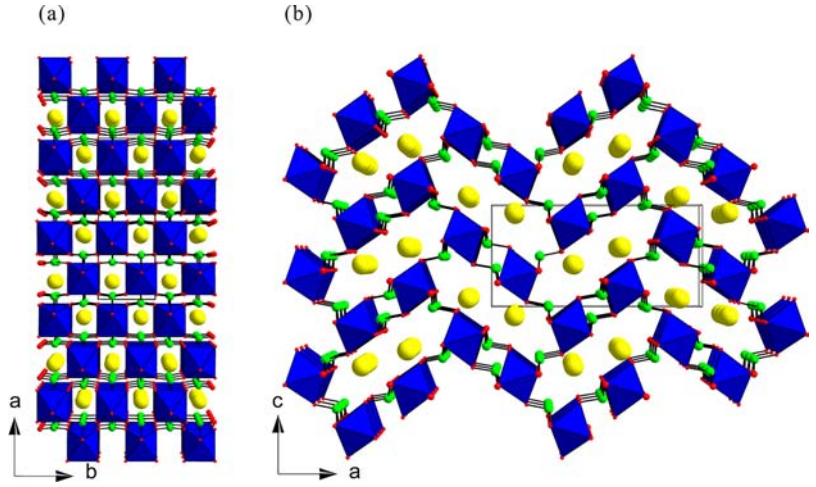

Figure 2. Ball-and-stick and polyhedral representations of $RbIn(SeO_3)_2$. (a) Four-membered ring channels running along the [001] direction are observed in the *ab*-plane. (b) Small 4-membered ring channels and large 12-membered ring channels composed of InO_6 octahedra and SeO_3 polyhedra are observed along the [010] direction in the *ac*-plane (blue, In; green, Se; yellow, Rb; red, O).

2.166(6) Å for $NaIn(SeO_3)_2$ and from 2.113(5) Å to 2.167(5) Å for $KIn(SeO_3)_2$. The O−In−O bond angles range from 81.1(6)° to 172.4(3)° for $NaIn(SeO_3)_2$ and 84.50(15)° to 173.84(15)° for $KIn(SeO_3)_2$. The two unique Se^{4+} cations are in distorted trigonal pyramidal environments, connected to three oxygen atoms. The Se−O bond lengths range from 1.658(8) Å to 1.700(9) Å for $NaIn(SeO_3)_2$ and 1.678(5) Å to 1.704(6) Å for $KIn(SeO_3)_2$. The Se^{4+} cations are in asymmetric coordination environments attributed to the stereoactive nonbonded electron pair. The Na^+ or K^+ cations are surrounded by eight oxygen atoms with Na−O or K−O contact distances ranging from 2.472(8) Å to 2.866(4) Å and from 2.747(4) Å to 2.9109(18) Å for $NaIn(SeO_3)_2$ and $KIn(SeO_3)_2$, respectively. All of the oxygen atoms in the corners of the InO_6 octahedra are shared by the SeO_3 polyhedra. Furthermore, each oxygen atom in the SeO_3 groups is shared by the InO_6 octahedra, which results in a three-dimensional framework structure. As can be seen in Figure 1b, 4-membered ring (4-MR) channels that are running along the [001] direction are observed in the *ab*-plane. Also, small 4-membered ring (4-MR) channels and large 12-membered ring (12-MR) channels composed of InO_6 octahedra and SeO_3 polyhedra are observed along the [010] direction in the *ac*-plane (see Figure 1c). Na^+ or K^+ cations are residing within the 12-MR channels. In connectivity terms, the structures of $NaIn(SeO_3)_2$ and $KIn(SeO_3)_2$ may be described as anionic frameworks of $\{[In(1)O_{6/2}]^{3-}\ [Se(1)O_{3/2}]^{1+}\ [Se(2)O_{3/2}]^{1+}\}^-$. Charge neutrality is maintained through the Na^+ or K^+ cation. Bond-valence calculations[32,33] for the In^{3+}, Se^{4+}, and Na^+ (or K^+) cations result in values in the range of 2.95−3.01, 3.80−4.17, and 0.91 (or 1.22), respectively.

$RbIn(SeO_3)_2$. Although $RbIn(SeO_3)_2$ crystallizes in the same centrosymmetric space group *Pnma* (No. 62) as those of $NaIn(SeO_3)_2$ and $KIn(SeO_3)_2$ with a similar framework, the framework structure is slightly different. The material consists of distorted InO_6 octahedra and SeO_3 groups connected by In−O−Se bonds. Similar to $NaIn(SeO_3)_2$ and $KIn(SeO_3)_2$, no In−O−In and Se−O−Se bonds are observed in the $RbIn(SeO_3)_2$. The In−O bond lengths and the O−In−O bond angles in a distorted octahedral coordination environment range from 2.134(2) Å to 2.177(2) Å and from 84.79(11)° to 177.48(13)°, respectively. The Se−O bond lengths in distorted trigonal pyramidal environments for the two unique Se^{4+} cations range from 1.687(3) Å to 1.695(3) Å. The Se^{4+} cations are in asymmetric coordination environments attributable to the stereoactive lone pairs. The Rb^+ cation is surrounded by eight oxygen atoms with Rb−O contact distances ranging from 2.959(2) Å to 3.0776(15) Å. $RbIn(SeO_3)_2$ exhibits a three-dimensional framework structure that is composed of the corner-shared InO_6 octahedra and the SeO_3 polyhedra. Similar to the structures of $NaIn(SeO_3)_2$ and $KIn(SeO_3)_2$, 4-membered ring (4-MR) channels running along the [001] direction are observed in the *ab*-plane (see Figure 2a). As seen in Figure 2b, small 4-membered ring (4-MR) channels and large 12-membered ring (12-MR) channels composed of InO_6 octahedra and SeO_3 polyhedra are observed along the [010] direction in the *ac*-plane as well. Within the 12-MR channels, Rb^+ cations are residing. However, the framework structure of $RbIn(SeO_3)_2$ is different to that of $NaIn(SeO_3)_2$ or $KIn(SeO_3)_2$. While the lone pairs on the SeO_3 groups in $NaIn(SeO_3)_2$ or $KIn(SeO_3)_2$ are oriented inward within the larger 12-MR channels, those observed in $RbIn(SeO_3)_2$ are pointing inward within the smaller 4-MR channels. As we will discuss in more detail later, the different framework structure of $RbIn(SeO_3)_2$ may be attributable to the larger size of the Rb^+ cation. In connectivity terms, the structure of $RbIn(SeO_3)_2$ may be described as an anionic framework of $\{[In(1)O_{6/2}]^{3-}\ [Se(1)O_{3/2}]^{1+}\ [Se(2)O_{3/2}]^{1+}\}^-$. The charge balance is maintained by incorporation of the Rb^+ cation. Bond valence calculations[32,33] for the In^{3+}, Se^{4+}, and Rb^+ result in values of 2.94, 3.85−3.91, and 0.88, respectively.

$CsIn(SeO_3)_2$. $CsIn(SeO_3)_2$ crystallizes in the trigonal centrosymmetric space group $R\bar{3}m$ (No. 166). The structure is composed of InO_6 octahedra and asymmetric SeO_3 polyhedra that are connected through oxygen atoms with In−O−Se bonds. $CsIn(SeO_3)_2$ also does not contain any In−O−In or Se−O−Se bonds. The In^{3+} cations are in a normal octahedral coordination environment, connected to six oxygen atoms with the In−O bond distances of 2.153(4) Å. The O−In−O bond angles range from 87.99(17)° to 180.0(2)°. The Se^{4+} cations are in distorted trigonal pyramidal environments, connected to three oxygen atoms. In examining the thermal ellipsoid for Se(1) in $CsIn(SeO_3)_2$, we determined that this atom could be split over two sites, Se(1) and Se(1′). In doing

dx.doi.org/10.1021/ic301316r | *Inorg. Chem.* 2012, 51, 8530−8537

so, fractional occupancies of 0.913(8) and 0.093(9) were refined, respectively. The Se−O bond lengths range from 1.623(6) Å to 1.695(4) Å for $CsIn(SeO_3)_2$. The Cs^+ cations are encompassed by 12 oxygen atoms with Cs−O contact distances of 3.417(3) Å in hexagonal prismatic environments. The InO_6 octahedra and the asymmetric SeO_3 polyhedra are sharing their corners through O(1) and are forming a layered structure (see Figure 3a). Huge Cs^+ cations are residing between the layers in order to make a charge balance. As we indicated earlier, the Se^{4+} cations are slightly disordered. Interestingly, more than 90% of the lone pairs on the disordered SeO_3 groups are pointing in the opposite direction of the large Cs^+ cation, where little space for lone pairs is available. Hexagonal six-membered rings (6-MRs) composed of both InO_6 octahedra and SeO_3 polyhedra are observed in the layer (see Figure 3b). Also, the SeO_3 groups link to the 6-MRs on both sides, above and below along the [001] direction. In connectivity terms, the structures of $CsIn(SeO_3)_2$ can be described as anionic layers of $\{[In(1)O_{6/2}]^{3-}\ 2[Se(1)O_{3/2}]^{1+}\}^{-}$. Charge neutrality is maintained by the Cs^+ cation. Bond valence calculations[32,33] for the In^{3+}, Se^{4+}, and Cs^+ cations result in values of 3.04, 4.18, and 0.80, respectively.

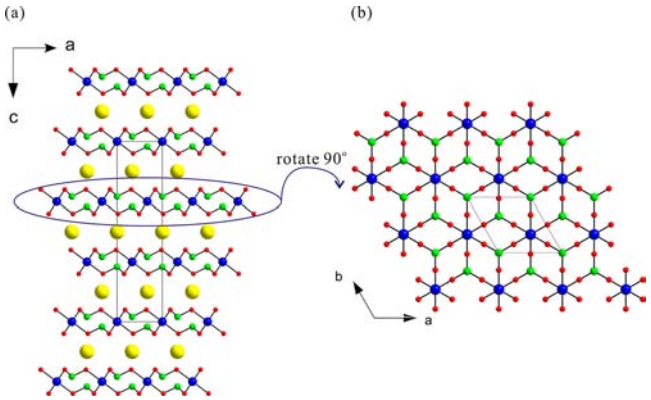

Figure 3. Ball-and-stick representations of $CsIn(SeO_3)_2$ (a) in the *ac*-plane and (b) in the *ab*-plane (blue, In; green, Se; yellow, Cs; red, O). For clarity, only one of the disordered Se^{4+} cations is shown. The InO_6 octahedra and the asymmetric SeO_3 polyhedra are sharing their corners through O(1) and are forming a layered structure. Cs^+ cations are residing between the layers to make a charge balance. Hexagonal six-membered rings (6-MRs) composed of both InO_6 octahedra and SeO_3 polyhedra are observed in the layer.

Infrared Spectroscopy. The infrared spectra of $AIn(SeO_3)_2$ (A = Na, K, Rb, and Cs) revealed several In−O and Se−O vibrations found in the region between 400 cm^{-1} and 860 cm^{-1}. Bands for In−O vibrations are observed at ~406−428 cm^{-1}. Multiple bands between 518 cm^{-1} and 858 cm^{-1} are attributed to the Se−O vibrations. The assignments are consistent with those previously reported.[20,22] The infrared spectra for the reported materials have been deposited in the Supporting Information.

Thermal Analysis. The thermal behaviors of the reported materials were investigated using thermogravimetric analysis (TGA) and powder X-ray diffraction (XRD). As indicated by the TGA diagram, $AIn(SeO_3)_2$ are thermally stable up to temperatures of ~520 °C. Above the temperature, the materials started to decompose, which may be attributable to the sublimation of SeO_2. Thermal decomposition products at 1000 °C in air for $AIn(SeO_3)_2$ resulted in In_2O_3 and some unknown amorphous phase as confirmed by powder XRD measurements. The TGA data have been deposited in the Supporting Information.

Influence of the Cation Size on the Framework Structures. All of the reported materials, $AIn(SeO_3)_2$ (A = Na, K, Rb, and Cs) are stoichiometrically equivalent. Although $NaIn(SeO_3)_2$ and $KIn(SeO_3)_2$ are isostructural, the other phases are not. However, all the reported phases share a common structural motif, a network of corner-shared InO_6 octahedra and SeO_3 groups. Each InO_6 octahedron is corner-shared, through oxygen, with six SeO_3 polyhedra. The alkali-metal cations occupy the respective cavities formed by the 12-membered rings and/or interlayer spaces. Interestingly, the size of the alkali-metal cation influences the nature of the SeO_3 group bonding mode to the InO_6 octahedra. Taken from Shannon,[34] the ionic radii for 8-coordinated Na^+, K^+, and Rb^+ and for 12-coordinated Cs^+ are 1.18, 1.51, 1.61, and 1.88 Å, respectively. Thus, in $NaIn(SeO_3)_2$ and $KIn(SeO_3)_2$, the lone pairs on the SeO_3 groups are pointing inward within the larger 12-MR channels, in which plenty of available spaces for the lone pairs are observed (see Figure 4a). In $RbIn(SeO_3)_2$, however, the lone pairs on the SeO_3 groups are pointing in opposite directions, compared to those of $NaIn(SeO_3)_2$ or $KIn(SeO_3)_2$, attributable to the larger size of the Rb^+ cation. In other words, it would be difficult to find any space for the lone

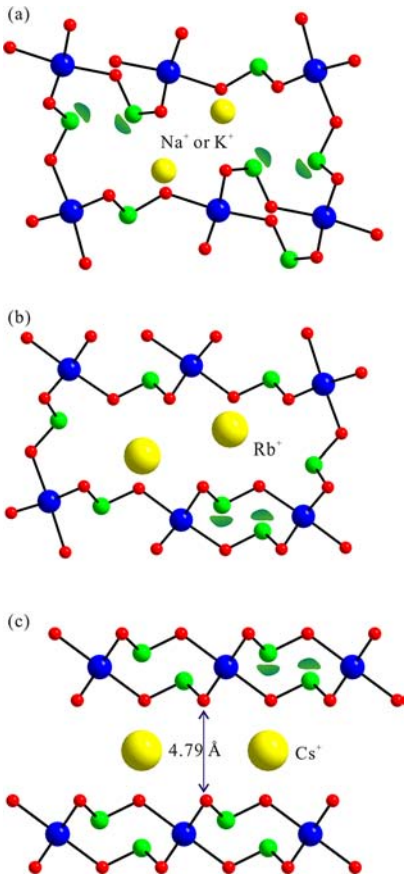

Figure 4. Ball-and-stick representations of the network of corner-shared InO_6 octahedra and SeO_3 groups in (a) $NaIn(SeO_3)_2$ or $KIn(SeO_3)_2$, (b) $RbIn(SeO_3)_2$, and (c) $CsIn(SeO_3)_2$ (blue, In; green, Se; yellow, Na, K, Rb, or Cs; red, O). The lone pair on Se^{4+} is drawn schematically and is not the result of the electron localization function (ELF) calculations.

dx.doi.org/10.1021/ic301316r | Inorg. Chem. 2012, 51, 8530−8537

pairs in the 12-MR channels, where larger Rb^+ cations are residing. Thus, the lone pairs on the SeO_3 groups in $RbIn(SeO_3)_2$ are pointing inward within the smaller 4-MR channels (see Figure 4b). Finally, the larger interlayer spacing in $CsIn(SeO_3)_2$ forces the Se^{4+} bond to three oxygen atoms only within one layer. While the nearest Se−O contact on an adjacent layer is at a distance of 2.63 Å, the closest interlayer O−O contact distance is 4.79 Å. Thus, all the largest Cs^+ cation should reside in the interlayer space and the framework of $CsIn(SeO_3)_2$ results in the 2D layered structure (see Figure 4c). A three-dimensional cesium indium selenite material, $CsH_2In_3(SeO_3)(H_2O)_2$[17] is observed in the literature, where the framework is similarly composed of InO_6 octahedra and SeO_3 polyhedra. However, in $CsH_2In_3(SeO_3)_6(H_2O)_2$, the amount of larger cation (Cs^+) residing in the A-cation sites is only one-third, compared to that of $CsIn(SeO_3)_2$. Thus, the interlayer spacing is not so much forced by the Cs^+, which results in a three-dimensional framework structure.

Dipole Moment Calculations. Although $AIn(SeO_3)_2$ (A = Na, K, Rb, and Cs) crystallize in centrosymmetric space groups, the materials contain a cation (Se^{4+}) that exhibits a local asymmetric environment attributable to the lone pair. One of our important motivations for investigating materials containing asymmetric lone-pair cations is to better understand the coordination environments. The direction and magnitude of the distortions in the SeO_3 polyhedra may be quantified by determining the local dipole moments. This approach has been described earlier, with respect to octahedra for metal oxyfluorides.[35,36] The method uses a bond valence approach to calculate the direction and magnitude of the local dipole moments. With the lone-pair polyhedra, the lone pair is given a charge of −2 and the localized Se^{4+} lone-pair distance is estimated to be 1.22 Å, based on the earlier work of Galy et al.[37] Using this methodology, the dipole moment for the SeO_3 polyhedra in the reported materials is in the range of ∼7.08−9.27 D (where D denotes Debyes). In fact, an examination of 36 examples of SeO_3 polyhedra found in indium selenites materials reveals that the dipole moments range from 6.99 D to 11.00 D, with an average value of 8.01 D. The values are consistent with those reported dipole moments for SeO_3 polyhedra.[25,26,38,39] A complete calculation of dipole moments for the SeO_3 polyhedra is listed in Table 3.

Ion-Exchange Experiments. The layered structural feature of $CsIn(SeO_3)_2$ suggested the material may be able to undergo ion-exchange reactions in which the Cs^+ cation is replaced by smaller cations. Our experiments revealed that $CsIn(SeO_3)_2$ displays robust ion-exchange behavior. It was possible to completely exchange the Cs^+ cation for Li^+ by heating $CsIn(SeO_3)_2$ with Li_2CO_3 in water to 200 °C for 5 days. After cooling to room temperature at a rate of 6 °C h^{-1}, colorless crystals of $LiIn(SeO_3)_2$ were obtained, which was identified by single-crystal XRD. Interestingly, the layered structure of $CsIn(SeO_3)_2$ transformed to the three-dimensional framework during the ion-exchange reaction (see Figure 5). No Cs^+ ion has been detected from the elemental analysis on the ion-exchanged crystals. The exchanged material crystallized in the rhombohedral space group, $R\bar{3}$, with $a = b = 9.3572(2)$ Å and $c = 26.1483(7)$ Å. Work is underway to confirm the phase purity as well as full characterization of the ion-exchanged material.

Table 3. Calculation of Dipole Moments for SeO_3 Polyhedra

SeO_3	dipole moment (D)
$Cs_3H_6In_5(SeO_3)_{12}$ (from ref 16)	
$Se(1)O_3$	9.51
$Se(2)O_3$	8.09
$Se(3)O_3$	8.64
$Se(4)O_3$	8.80
$Se(5)O_3$	7.53
$Se(6)O_3$	8.56
$CsIn_3H_2(SeO_3)_6(H_2O)_2$ (from ref 17)	
$Se(1)O_3$	8.37
$Se(2)O_3$	8.97
$Se(3)O_3$	11.00
$Se(4)O_3$	7.76
$In(HSeO_3)(SeO_3)$ (from ref 18)	
$Se(1)O_3$	8.27
$Se(2)O_3$	8.10
$In_2(Se_2O_5)_3$ (from ref 20)	
$Se(1)O_3$	8.59
$Se(2)O_3$	8.15
$Se(3)O_3$	7.09
$Se(4)O_3$	8.46
$Se(5)O_3$	7.42
$Se(6)O_3$	7.70
$Se(7)O_3$	8.40
$Se(8)O_3$	7.24
$Se(9)O_3$	8.22
$Se(10)O_3$	8.40
$Se(11)O_3$	7.24
$Se(12)O_3$	8.22
$In(OH)(SeO_3)$ (from ref 21)	
$Se(1)O_3$	6.99
$Se(2)O_3$	7.28
$In_2Cu_3(SeO_3)_6$ (from ref 22)	
$Se(1)O_3$	8.04
$Se(2)O_3$	7.66
$Se(3)O_3$	7.97
$[In_2(SeO_3)_2(C_2O_4)(H_2O)_2]\cdot 2H_2O$ (from ref 23)	
$Se(1)O_3$	7.83
$In_2Mo_2Se_2O_{13}(H_2O)$ (from ref 24)	
$Se(1)O_3$	8.05
$InSeO_3Cl$ (from ref 25)	
$Se(1)O_3$	7.43
$InVSe_2O_8$ (from ref 26)	
$Se(1)O_3$	7.43
$Se(2)O_3$	7.09
$Se(3)O_3$	7.87
$Se(4)O_3$	7.50
$NaIn(SeO_3)_2$ (this work)	
$Se(1)O_3$	9.27
$Se(2)O_3$	7.56
$KIn(SeO_3)_2$ (this work)	
$Se(1)O_3$	8.01
$Se(2)O_3$	7.45
$RbIn(SeO_3)_2$ (this work)	
$Se(1)O_3$	8.14
$Se(2)O_3$	7.20
$CsIn(SeO_3)_2$ (this work)	
$Se(1)O_3$	7.08
average	8.01

dx.doi.org/10.1021/ic301316r | Inorg. Chem. 2012, 51, 8530−8537

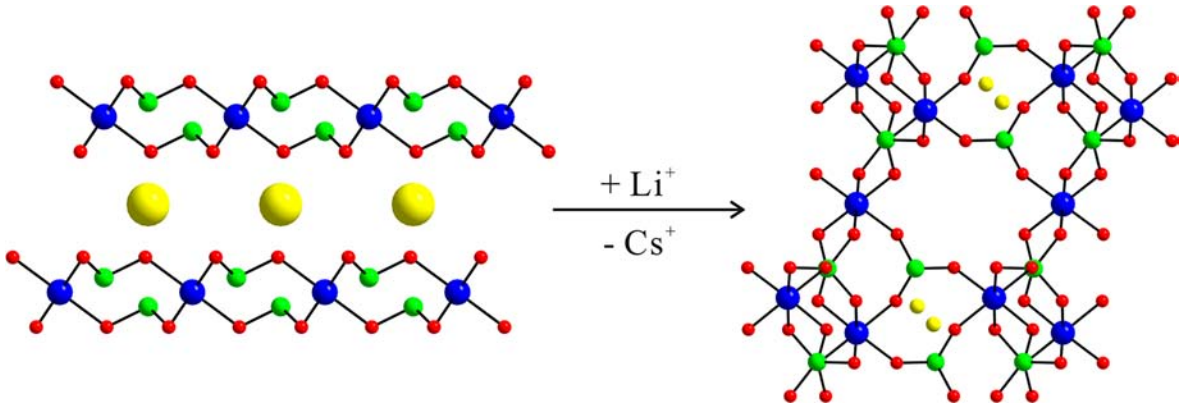

Figure 5. Ball-and-stick representations for the ion-exchange reaction of $CsIn(SeO_3)_2$ with Li^+ cation. Note how the layered structure transforms to the three-dimensional framework structure during the ion-exchange reaction.

CONCLUSIONS

We have successfully synthesized a series of new quaternary mixed-metal selenites materials, $AIn(SeO_3)_2$ (A = Na, K, Rb, and Cs) by standard solid-state and hydrothermal reactions. Although the reported materials are stoichiometrically equivalent, crystallographic data indicate that $NaIn(SeO_3)_2$, $KIn(SeO_3)_2$, and $RbIn(SeO_3)_2$ exhibit three-dimensional framework structures, whereas $CsIn(SeO_3)_2$ possesses a layered structure. Detailed structural analyses suggest that the cation size plays an important role in determining the framework structures of the materials. The dipole moment calculations, infrared spectroscopy, and thermal analysis have been obtained for the new materials. Further syntheses with other local asymmetric building blocks are ongoing and will be reported shortly.

ASSOCIATED CONTENT

Supporting Information

X-ray crystallographic file in CIF format, calculated and observed X-ray diffraction patterns, thermogravimetric analysis diagrams, infrared spectra, ORTEP representations for $AIn(SeO_3)_2$ (A = Na, K, Rb, and Cs). This material is available free of charge via the Internet at http://pubs.acs.org.

AUTHOR INFORMATION

Corresponding Author

*Tel.: +82-2-820-5197. Fax: +82-2-825-4736. E-mail: kmok@cau.ac.kr.

Notes

The authors declare no competing financial interest.

ACKNOWLEDGMENTS

This research was supported by Basic Science Research Program through the National Research Foundation of Korea (NRF) funded by Ministry of Education, Science & Technology (Grant No. 2010-0002480).

REFERENCES

(1) Jona, F.; Shirane, G. *Ferroelectric Crystals*; Pergamon Press: Oxford, U.K., 1962.
(2) Cady, W. G. *Piezoelectricity: An Introduction to the Theory and Applications of Electromechanical Phenomena in Crystals*; Dover: New York, 1964.
(3) Lang, S. B. *Sourcebook of Pyroelectricity*; Gordon & Breach Science: London, 1974.
(4) Lines, M. E.; Glass, A. M. *Principles and Applications of Ferroelectrics and Related Materials*; Oxford University Press: Oxford, U.K., 1991.
(5) Gillespie, R. J.; Nyholm, R. S. *Q. Rev., Chem. Soc.* **1957**, *11*, 339.
(6) Orgel, L. E. *J. Chem. Soc.* **1959**, 3815.
(7) Seshadri, R.; Hill, N. A. *Chem. Mater.* **2001**, *13*, 2892.
(8) Opik, U.; Pryce, M. H. L. *Proc. R. Soc. London, A* **1957**, *A238*, 425.
(9) Bader, R. F. W. *Mol. Phys.* **1960**, *3*, 137.
(10) Bader, R. F. W. *Can. J. Chem.* **1962**, *40*, 1164.
(11) Pearson, R. G. *J. Mol. Struct.: THEOCHEM* **1983**, *103*, 25.
(12) Wheeler, R. A.; Whangbo, M.-H.; Hughbanks, T.; Hoffmann, R.; Burdett, J. K.; Albright, T. A. *J. Am. Chem. Soc.* **1986**, *108*, 2222.
(13) Halasyamani, P. S.; Poeppelmeier, K. R. *Chem. Mater.* **1998**, *10*, 2753.
(14) Wickleder, M. S. *Chem. Rev.* **2002**, *102*, 2011.
(15) Ok, K. M.; Halasyamani, P. S. *Angew. Chem., Int. Ed.* **2004**, *43*, 5489.
(16) Mukhtarova, N. N.; Kalinina, V. P.; Rastsvetaeva, R. K.; Ilyukhin, V. V.; Belov, N. V. *Dokl. Akad. Nauk SSSR* **1980**, *254*, 359.
(17) Rastsvetaeva, R. K.; Andrianov, V. I.; Volodina, A. N. *Dokl. Akad. Nauk SSSR* **1984**, *277*, 871.
(18) Harrison, W. T. A.; Stucky, G. D.; Cheetham, A. K. *Eur. J. Solid State Inorg. Chem.* **1993**, *30*, 347.
(19) Yaroslavtsev, A. B.; Nikolaev, A. E.; Ilyukhin, A. B.; Chuvaev, V. F. *Zh. Neorg. Khim.* **1996**, *41*, 1616.
(20) Ok, K. M.; Halasyamani, P. S. *Chem. Mater.* **2002**, *14*, 2360.
(21) Paterson, B.; Harrison, W. T. A. *Z. Anorg. Allg. Chem.* **2007**, *633*, 158.
(22) Kong, F.; Lin, Q.; Yi, F. Y.; Mao, J. G. *Inorg. Chem.* **2009**, *48*, 6794.
(23) Cao, J.; Li, G.; Chen, J. *J. Solid State Chem.* **2009**, *182*, 102.
(24) Kong, F.; Hu, C.; Hu, T.; Zhou, Y.; Mao, J. G. *Dalton Trans.* **2009**, *2009*, 4962.
(25) Lee, D. W.; Ok, K. M. *Solid State Sci.* **2010**, *12*, 2036.
(26) Lee, D. W.; Oh, S.-J.; Halasyamani, P. S.; Ok, K. M. *Inorg. Chem.* **2011**, *50*, 4473.
(27) *SAINT, Program for Area Detector Absorption Correction*; version 4.05; Siemens Analytical X-ray Instruments: Madison, WI, USA, 1995.
(28) Blessing, R. H. *Acta Crystallogr., Sec. A: Found. Crystallogr.* **1995**, *A51*, 33.
(29) Sheldrick, G. M. *SHELXS-97—A program for automatic solution of crystal structures*; University of Goettingen: Goettingen, Germany, 1997.
(30) Sheldrick, G. M. *SHELXL-97—A program for crystal structure refinement*; University of Goettingen: Goettingen, Germany, 1997.
(31) Farrugia, L. J. *J. Appl. Crystallogr.* **1999**, *32*, 837.
(32) Brown, I. D.; Altermatt, D. *Acta Crystallogr., Sect. B: Struct. Sci.* **1985**, *B41*, 244.
(33) Brese, N. E.; O'Keeffe, M. *Acta Crystallogr., Sect. B: Struct. Sci.* **1991**, *B47*, 192.

(34) Shannon, R. D. *Acta Crystallogr., Sect. A: Cryst. Phys., Diffr., Theor. Gen. Crystallogr.* **1976**, *A32*, 751.
(35) Maggard, P. A.; Nault, T. S.; Stern, C. L.; Poeppelmeier, K. R. *J. Solid State Chem.* **2003**, *175*, 25.
(36) Izumi, H. K.; Kirsch, J. E.; Stern, C. L.; Poeppelmeier, K. R. *Inorg. Chem.* **2005**, *44*, 884.
(37) Galy, J.; Meunier, G. *J. Solid State Chem.* **1975**, *13*, 142.
(38) Oh, S.-J.; Lee, D. W.; Ok, K. M. *Inorg. Chem.* **2012**, *51*, 5393.
(39) Oh, S.-J.; Lee, D. W.; Ok, K. M. *Dalton Trans.* **2012**, *41*, 2995.